ΔT14/ΔD15 *Azotobacter vinelandii* Ferredoxin I: Creation of a New CysXXCysXXCys Motif That Ligates a [4Fe-4S] Cluster†

Mary A. Kemper,‡ H. Samantha Gao-Sheridan,‡ Binghui Shen,‡,§ Jillian L. C. Duff,|| Gareth J. Tilley,|| Fraser A. Armstrong,|| and Barbara K. Burgess*,‡

Department of Molecular Biology and Biochemistry, University of California, Irvine, California 92697-3900, and Department of Chemistry, Oxford University, Oxford, U.K.

Received May 6, 1998; Revised Manuscript Received June 29, 1998

ABSTRACT: In clostridial-type ferredoxins, each of the two [4Fe-4S]$^{2+/+}$ clusters receives three of its four ligands from a CysXXCysXXCys motif. *Azotobacter vinelandii* ferredoxin I (*Av*FdI) is a seven-iron ferredoxin that contains one [4Fe-4S]$^{2+/+}$ cluster and one [3Fe-4S]$^{+/0}$ cluster. During the evolution of the 7Fe azotobacter-type ferredoxins from the 8Fe clostridial-type ferredoxins, one of the two motifs present changed to a CysXXCysXXXXCys motif, resulting in the inability to form a 4Fe cluster and the appearance of a 3Fe cluster in that position. In a previous study, we were unsuccessful in using structure as a guide in designing a 4Fe cluster in the 3Fe cluster position of *Av*FdI. In this study, we have reversed part of the evolutionary process by deleting two residues between the second and third cysteines. UV/Vis, CD, and EPR spectroscopies and direct electrochemical studies of the purified protein reveal that this ΔT14/ΔD15 FdI variant is an 8Fe protein containing two [4Fe-4S]$^{2+/+}$ clusters with reduction potentials of −466 and −612 mV versus SHE. Whole-cell EPR shows that the protein is present as an 8Fe protein in vivo. These data strongly suggest that it is the sequence motif rather than the exact sequence or the structure that is critical for the assembly of a 4Fe cluster in that region of the protein. The new oxygen-sensitive 4Fe cluster was converted in partial yield to a 3Fe cluster. In known ferredoxins and enzymes that contain reversibly interconvertible [4Fe-4S]$^{2+/+}$ and [3Fe-4S]$^{+/0}$ clusters, the 3Fe form always has a reduction potential ca. 200 mV more positive than the 4Fe cluster in the same position. In contrast, for ΔT14/ΔD15 FdI, the 3Fe and 4Fe clusters in the same location have extremely similar reduction potentials.

Azotobacter vinelandii ferredoxin I (*Av*FdI)[1] is one member of a class of proteins found in aerobic organisms that contain one [3Fe-4S]$^{+/0}$ cluster and one [4Fe-4S]$^{2+/+}$ cluster. These proteins are believed to have evolved from a class of ferredoxins found in anaerobic bacteria that contain two [4Fe-4S]$^{2+/+}$ clusters (*1*). As shown in Figure 1 sequence comparisons of these and many other [Fe-S] proteins have revealed a highly conserved CysXXCysXX-CysXXXCysPro motif associated with the presence of a [4Fe-4S]$^{2+/+}$ cluster. Indeed, the detection of this motif in the sequence of an unknown protein, or a protein whose cluster type is unknown, is usually interpreted as evidence that a [4Fe-4S]$^{2+/+}$ cluster is present [for reviews, see *2*−*7*].

It is likely that during the evolution of the 7Fe ferredoxins from the 8Fe ferredoxins one of the two motifs present changed to a CysXXCysXXXXCysXXXCysPro motif (Figure 2) (*1*). This change involved the insertion of two residues between the second and third cysteines. Comparison of the X-ray structures of 8Fe and 7Fe proteins (*8*−*14*) shows that this insertion moved the second cysteine out of reach of the cluster, resulting in the inability to form a [4Fe-4S]$^{2+/+}$ cluster and the appearance of a [3Fe-4S]$^{+/0}$ cluster in that position. As shown in Figure 2, evolution in some organisms led to the removal of the second cysteine altogether by converting that residue to valine. Another difference between the two classes of proteins is that the *Av*FdI-type ferredoxins are twice as large as the clostridial-type ferredoxins. This change in size results from a C-terminal extension that wraps around the [3Fe-4S] portion of the protein.

Very little is known about how [Fe-S] clusters are assembled in vivo and the extent to which the sequence motif is important in directing the cluster assembly process. In a previous study, we used structure as a guide and designed a Y13C variant of FdI that could easily be modeled with a [4Fe-4S] cluster in the [3Fe-4S] cluster position (*15*). That mutation, which was based on structural comparisons of 7Fe and 8Fe ferredoxins, did not introduce the CysXXCysXX-CysXXXCysPro motif and did not result in the formation of a new [4Fe-4S] cluster. In this study, we attempted to reverse part of the evolutionary process by removing two residues between Cys^{11} and Cys^{16} using site-directed mutagenesis. This ΔT14/ΔD15 *Av*FdI mutation restored a classic [4Fe-4S] Cys^{8}XXCys^{11}XXCys^{14}XXXCysPro motif in the [3Fe-4S]$^{+/0}$ cluster region of the protein while leaving

† This work was supported by National Institutes of Health Grant GM-45209 to B.K.B. and by grants from UK EPSRC GR/J84809 to F.A.A.

* To whom correspondence should be addressed: (949) 824-4297 (phone), (949) 824-8551 (FAX), or bburgess@uci.edu (e-mail).

‡ University of California, Irvine.

§ Current address: Cell & Tumor Biology, City of Hope, 1500 E. Duarte Rd., Duarte, CA 91010.

|| Oxford University.

[1] Abbreviations: *Av*FdI, *Azotobacter vinelandii* ferredoxin I; CD, circular dichroism; EPR, electron paramagnetic resonance; SCE, saturated calomel electrode; SHE, standard hydrogen electrode.

S0006-2960(98)01049-6 CCC: $15.00 © 1998 American Chemical Society
Published on Web 08/21/1998

***Cp*Fd**	IADS**C**VS**C**GA**C**ASE**CP**VNAIS	***E. coli* DMSR**	DSSR**C**TG**C**KT**C**ELA**C**KDYKDL
***Cp*Fd^1**	DADT**C**ID**C**GN**C**ANV**CP**VGAPV	***E. coli* DMSR^1**	DEDV**C**IG**C**RY**C**HMA**CP**YGAPQ
***Ca*Fd**	INEA**C**IS**C**GA**C**EPE**CP**VNAIS	***Mf*FdH**	DFSR**C**LK**C**YG**C**REA**CP**ICYCE
***Ca*Fd^1**	DADT**C**ID**C**GA**C**AGV**CP**VDAPV	***Mf*FdH^1**	MVES**C**TN**C**GQ**C**EEV**CP**GEIPL
***Pa*Fd**	INDS**C**IA**C**GA**C**KPE**CP**VNCIQ	**Human SDH**	GLYE**C**IL**C**AC**C**STS**CP**SYWWN
***Pa*Fd^1**	DADS**C**ID**C**GS**C**ASV**CP**VGAPN	**Tobacco PsaC**	IYDT**C**IG**C**TQ**C**VRA**CP**TDVLE
***Mt*Fd**	NADE**C**SG**C**GS**C**VDE**CP**SEAIT	**Tobacco PsaC^1**	RTED**C**VG**C**KR**C**ESA**CP**TDFLS
***Mt*Fd^1**	DQDE**C**VE**C**GA**C**EEA**CP**NQAIK	**Bovine NADHDH**	GEER**C**IA**C**KL**C**EAV**CP**AQAIT
***Cp*Hyd**	DRTK**C**LL**C**GR**C**VNA**C**GKNTET	**Bovine NADHDH^1**	DMTK**C**IY**C**GF**C**QEA**CP**VDAIV
***Cp*Hyd^1**	DDTN**C**LL**C**GQ**C**IIA**CP**VAALS	***Anabaena* PatB**	PNNS**C**VG**C**DN**C**RPQ**CP**TGAIK

FIGURE 1: Comparison of the sequences for a number of [4Fe-4S] cluster containing proteins that have the CysXXCysXXCysXXXCysPro motif (*60*). *Cp, Clostridium pasteurianum*; *Ca, Clostridium acidurici; Pa, Peptostreptococcus asaccharolyticus; Mt, Methanosarcina thermophila; Mf, methanbacterium formicicum;* Fd*;* ferredoxin; Hyd, hydrogenase; DMSR, dimethyl sulfoxide reductase; FDH, formate dehydrogenase; SDH, succinate−ubiquinone oxidoreductase; PsaC, chloroplast photosystem I subunit Psa C; NADHDH, NADH dehydrogenase; PatB, putative transcriptional regulator. The superscripted 1 indicates the second motif in the same protein.

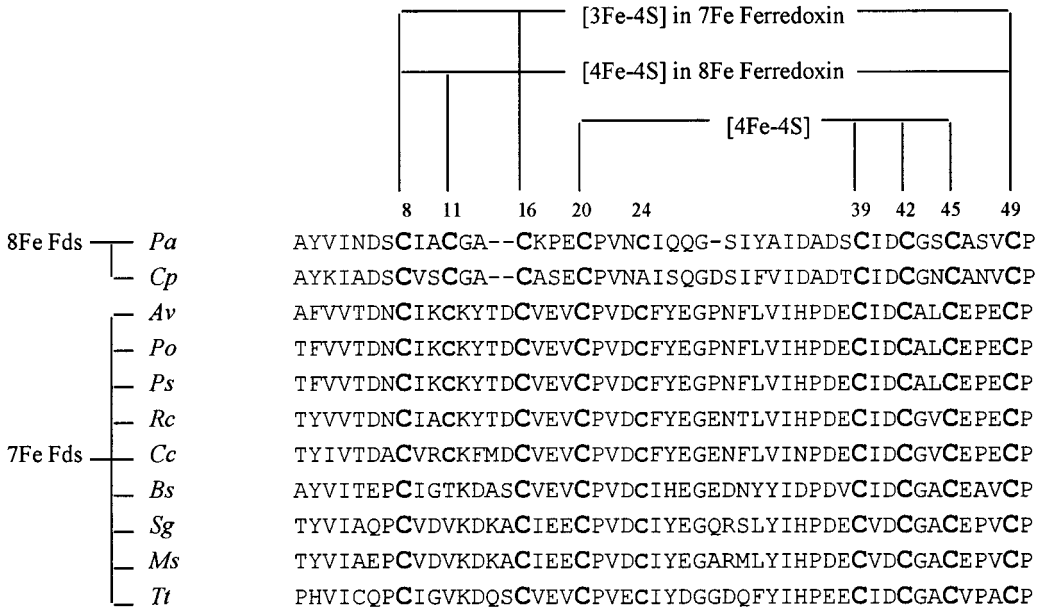

FIGURE 2: Sequence comparison of *Av*FdI to the 8Fe ferredoxins of *P. aerogenes* and *C. pasteurianum* and to other 7Fe ferredoxins. *Pa, Peptococcus aerogenes* Fd (*13*); *Cp, Clostridium pasteurianum* Fd (*61*); *Av, A. vinelandii* FdI (*18*); *Po, Pseudomonas ovalis* Fd II (*62*); *Ps, Pseudomonas stutzeri* Fd (*63*); *Rc, Rhodobacter capsulatus* Fd II (*64*); *Cc, Caulobacter crescentus* Fd (*65*); *Bs, Bacillus schlegelii* (*66*); *Sg, Streptomyces griseus* Fd (*67*); *Tt, Thermus thermophilus* Fd (*68*).

the protein twice as long as the clostridial-type ferredoxins. Here we report the purification and characterization of ΔT14/ΔD15 FdI.

MATERIALS AND METHODS

Materials. Native *Av*FdI was purified as described previously (*16*). Ammonium sulfate was from Fisher, and all other materials were obtained from the vendors listed previously (*17*).

Mutagenesis of fdxA, Expression and Purification of ΔT14/ΔD15 FdI. The oligonucleotide used for the mutagenesis had the sequence ATCAAGTGCAAGTACTGTGTTGAAGTCTGC. This sequence differs from the wild-type sequence (*18*) by the deletion of the six bases that encode T14 and D15 within the *fdx*A gene, resulting in the deletion of those two residues in the protein. The success of the mutagenesis was confirmed at the DNA level by dideoxy-DNA sequencing and at the protein level by NH_2-terminal protein sequencing that was carried out in the protein sequencing facility in the Department of Molecular Biology and Biochemistry at UCI. Unless otherwise indicated, oligonucleotide-directed in vitro mutagenesis, FdI overexpression, cell growth, and Western analysis were performed as described previously (*17*). The purification of ΔT14/ΔD15 FdI was carried out anaerobically and is a modification of purification method 2 described by Stephens et al. (*16*). *A. vinelandii* strain JG100 has a deletion in the *fdx*A gene and does not synthesize FdI. *A. vinelandii* JG100 containing the overexpression vector for ΔT14/ΔD15 FdI was grown under nitrogen-fixing conditions, and cell-free extracts were prepared from 1 kg of cell paste. The cell-free extracts were not heat-treated as described in the purification of nitrogenase (*19*) due to the possibility that the mutant protein could be heat-labile. All steps were carried out anaerobically with 2 mM $Na_2S_2O_4$ present in all buffers. Cell-free extracts were loaded onto a 5 cm × 20 cm DE-52 cellulose column equilibrated with 0.025 M Tris-HCl, pH 7.4. Following loading and washing, the column was chromatographed with a 0.1−0.5 M NaC1 linear gradient (2 L of each, 570 mL/h) in the same buffer. ΔT14/ΔD15 FdI was eluted completely at a salt concentration of 0.43 M NaC1. The ferredoxin fraction was immediately diluted 1:2 in 0.1 M potassium

phosphate buffer, pH 7.4, and loaded onto a 2.5 cm × 10 cm DE-52 cellulose column equilibrated with the same buffer. After loading, the column was washed with 4 L of 0.1 M potassium phosphate buffer, pH 7.4, 0.12 M in KC1, at a rate of 300 mL/h. A gradient from 0.12 to 0.3 M KC1 (800 mL of each) followed, and ΔT14/ΔD15 FdI eluted close to 0.3 M KC1. Coomassie blue stained SDS−PAGE and Western immunoblotting were utilized to confirm the presence of mutant FdI. The FdI fraction was again diluted 1:2 in potassium phosphate buffer, pH 7.4, and concentrated on a 0.5 cm × 5 cm column. FdI eluted in a very concentrated form with 0.5 M NaC1, and a 10 mL sample was loaded onto a 2.5 cm × 100 cm Sephadex G-75 superfine gel filtration column equilibrated with 0.025 M Tris-HCl, pH 7.4, 0.1 M NaC1. A total of 40 mL of 70−80% saturated ammonium sulfate in 0.1 M Tris-HCl, pH 7.4, was added to 13 mL of ΔT14/ΔD15 FdI from the gel filtration column, slowly with stirring. The protein precipitated over the course of 2 h and was centrifuged in air-tight centrifuge tubes in a SS34 rotor at 6000 rpm for 35 min. The A_{280}/A_{400} ratio of oxidized ΔT14/ΔD15 FdI following ammonium sulfate precipitation for different preparations ranged from 1.6 to 1.8, and the A_{280}/A_{260} ratio ranged from 1.05 to 1.2.

Growth Curves. Fifty microliters of 130 Klett unit (mid log phase) growing cultures was used to inoculate 500 mL flasks containing 200 mL of Burks' media. All cultures were grown under nitrogen-fixing conditions with 0.1 μg/mL streptomycin present to maintain the pKT230 expression plasmid. The cultures were grown at 30 °C with a shaking rate of 150 rpm.

Spectroscopy. For spectroscopic studies, all protein samples were prepared anaerobically under Ar in a Vacuum Atmospheres glovebox (O_2 < 1 ppm) using degassed buffers. Where indicated, samples were first concentrated using a Centricon-10 microconcentrator and then buffer-exchanged into 0.025 mM Tris-HCl, pH 7.4. EPR spectra were obtained using a Bruker 300 Ez spectrometer, interfaced with an Oxford Instrument ESR-9002 liquid helium continuous flow cryostat. Samples for whole-cell EPR were prepared as follows: 100 mL cultures were grown to mid-log phase (120−150 Klett units) under nitrogen-fixing conditions with 0.4 μg/mL streptomycin present, at 30 °C with shaking at 200 rpm. The cultures were centrifuged at 2000*g* for 10 min. The pellets were then resuspended in 0.05 M Tris-HCl, pH 7.4, with 2.5 mL of buffer per gram of cell pellet, before transferring to EPR tubes for immediate freezing in liquid nitrogen. CD spectra were obtained using a JASCO J720 spectropolarimeter, and UV/Vis spectra were obtained with a HP 8452A Diode Array UV/Vis spectrophotometer.

Iron Content Analysis. To determine Fe content, samples were digested, and the analysis was carried out as described elsewhere (*19*) using $FeCl_3 \cdot 6H_2O$ to generate a standard curve with the native FdI and FdIII as controls. The concentrations of proteins were determined based on the extinction coefficients of 29 800 M^{-1} cm^{-1} at 400 nm for FdI and 31 200 M^{-1} cm^{-1} at 390 nm for FdIII.

Electrochemistry. DC cyclic voltammetry was carried out with an Autolab electrochemical analyzer (EcoChemie, Utrecht, The Netherlands). Electrochemical cells were of all-glass construction; either a single pot cell for bulk solution voltammetry or a multipot cell for protein film experiments, procedures for which have been described previously (*20*). The sample compartment was thermostated at 0 °C to optimize stability. The reference was a saturated calomel electrode (SCE) kept at 22 °C and held in a sidearm linked to the sample compartment by a luggin capillary. Potentials were converted to the Standard Hydrogen Electrode (SHE) by adding 243 mV from the measured E (SCE) (*21*). The PGE electrode (area approximately 0.18 cm^2) was prepared for protein application by polishing with an aqueous alumina slurry (Buehler Micropolish: 1.0 μm for protein film voltammetry or 0.3 μm for solution electrochemistry) and sonicated extensively in water to remove traces of Al_2O_3.

All electrochemical experiments were carried out using deionized water (Millipore 18 MΩ·cm) and analytical-grade reagents, and (as far as was practical) operations were carried out in a glovebox (Belle Technology, Dorset, England) with O_2 < 2 ppm. Before experiments, protein samples were chromatographed anaerobically by FPLC (Pharmacia) using a Mono-Q column. For bulk solution electrochemistry, protein concentrations were typically 100 μM in 20 mM HEPES, 0.1 M NaCl, 0.1 mM EGTA, with 3 mM neomycin (Sigma) to promote and stabilize the electrochemical response (*22*). For protein-film voltammetry, the cell contained either a 60 mM mixed-buffer system (consisting of 15 mM each of acetate, MES, HEPES, and TAPS) or 20 mM HEPES, each adjusted to the required pH, with either NaOH or HCl, 0.1 M NaCl as supporting electrolyte, and 0.1 mM EGTA. The cell also contained 200 μg/mL polymyxin to maintain equilibrium with polymyxin in the film (*22*). To prepare films, a ca. 1 μL aliquot of ice-cold ferredoxin solution (typically 100 μM in the 60 mM mixed buffer, pH 7.0, 0.1 M NaCl, 0.1 mM EGTA, with 200 μg/mL polymyxin as coadsorbate) was applied to the surface of the electrode with a fine glass capillary tip. Voltammograms were scanned first in a pot containing buffer−electrolyte at pH 7.0 in order to establish the film, following which the coated electrode could be transferred to other pots containing solutions at different pH.

RESULTS AND DISCUSSION

Mutation Design. The $[3Fe\text{-}4S]^{+/0}$ cluster of *Av*FdI is ligated by cysteinyl residues at positions 8, 16, and 49. As shown in Figure 2, there is also a free cysteine in the vicinity of the cluster at position 11. In an earlier study, we designed a Y13C variant of FdI based on stereochemical analysis of the structures of *Av*FdI and the clostridial-type 8Fe ferredoxins (*15*). That design strategy did not introduce a 4Fe cluster CysXXCysXXCysXXXCysPro binding motif but could easily be modeled with a 4Fe cluster in the 3Fe cluster position. Suprisingly, however, that design strategy was unsuccessful in creating the formation of a $[4Fe\text{-}4S]^{2+/+}$ cluster, and Y13C FdI retained its $[3Fe\text{-}4S]^{+/0}$ cluster.

In the current study, our strategy in generating the formation of a $[4Fe\text{-}4S]^{2+/+}$ cluster was to modify the $[3Fe\text{-}4S]^{+/0}$ cluster-associated sequence to a highly conserved $[4Fe\text{-}4S]^{2+/+}$ cluster-binding Cys motif. This motif, ^{8}CysXX-^{11}CysXX^{14}Cys, is shared by 8Fe ferredoxins from *Peptococcus aerogenes*, *Clostridium pasteurianum*, and other organisms, and provides three of the four ligands to a $[4Fe\text{-}4S]^{2+/+}$ cluster (Figure 2). To create this sequence motif in the vicinity of the *Av*FdI $[3Fe\text{-}4Fe]^{+/0}$ cluster, a ΔT14/ΔD15 variant of FdI was constructed and overexpressed in its native

background in *A. vinelandii.* Although this mutation introduced the correct sequence motif, it did not introduce the Ala and/or Gly residues that are normally found as residues between the Cys (Figures 1 and 2). In addition, *Av*FdI has an extended C-terminus which makes it twice as long as the clostridial ferredoxins. This C-terminus wraps around the $[3Fe\text{-}4S]^{+/0}$ portion of the protein and was also expected to influence the formation of a $[4Fe\text{-}4S]^{2+/+}$ cluster in that position.

Careful examination of the native structure leads to the conclusion that the formation of a stable 8Fe protein in the ΔT14/ΔD15 mutant of FdI is counter-intuitive, and we are unable to model such a mutation. Deletion of these residues requires that a significant rearrangement in the structure occurs. In native FdI, the carbonyl carbon atoms of Tyr13 and Asp15 are 5.7 Å apart, but in the ΔT14/ΔD15 mutant these atoms must superpose in order to form a new peptide bond between Tyr13 and Cys16. This could occur in one of two possible ways. (1) If the gap is closed entirely due to translation of Tyr13, then the chain of residues preceding Tyr13 must also translate. This would require conformational change of the residues in the cluster-binding loop Cys8-Ile9-Lys10-Cys11-Lys12-Tyr13. Ile9 is in contact with Phe31; Lys10 is solvent-exposed; Cys11 is in contact with Asn7, Ala91, Asp94, and Lys100; Lys12 is in contact with Glu27 and Gly28; and Tyr13 is in contact with Asp95. Also, the main chain atoms of these residues form hydrogen bonds with Asp6, Cys8, and Asn30 carbonyls and Lys84 and Lys100 side chains. Therefore, a number of favorable hydrophobic contacts, hydrogen bonds, and charged hydrogen bonds would have to be disrupted for the rearrangement to occur. Not only would favorable interactions be lost, but also new ones would have to be formed in the non-native conformation. One of these could be a bond between the side chain of Cys11 and the new [4Fe-4S] cluster. However, in the structure of the C20A mutant of FdI, this kind of new bond formation is only known to induce the inversion of a single peptide on the protein surface in concert with shifts of only about 1 Å in the surrounding residues (*24*). (2) If the gap is closed entirely by a shift of Cys16, then the helix of residues 17−19 would have to be extended. Cys20 is bonded to the [4Fe-4S] cluster; Glu18 is on the surface of the protein; and Val17 and Val19 have contacts on the interior with Phe25 and Cys45, respectively. While this rearrangement would involve fewer lost contacts and required new contacts, it would also result in a significant repositioning of Cys16 as a ligand to the new [4Fe-4S] cluster. Therefore, the extent of rearrangement that must occur is extensive in view of the structure of the native protein. In reality, residues on both sides of the gap would have to undergo substantial conformational change.

Consistent with this structural prediction, Western analysis of cell-free extracts and purification results revealed that the in vivo stability of ΔT14/ΔD15 FdI was much lower than for the native or surface residue variants of FdI (*23*) but similar to the stability of proteins resulting from mutations of cluster ligands that exhibited structural rearrangements (*24*, *25*). A further indication that a significant structural change has occurred is the observation that unlike all but one of the *Av*FdI variants reported to date (*15*, *17*, *23*−*25*) ΔT14/ΔD15 FdI failed to crystallize in either the triclinic form used for normal purification or the tetragonal form used for crystallography (*9*, *10*, *16*). Thus, at present no X-ray structure is available for ΔT14/ΔD15 FdI.

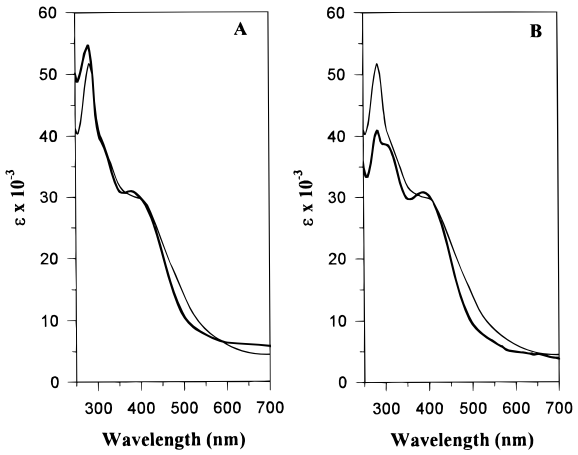

FIGURE 3: UV−visible absorption spectra of oxidized (A) native *Av*FdI (thin line) and ΔT14/ΔD15 FdI (thick line), 30 μM each, and (B) native *Av*FdI (thin line), 30 μM, and the 8Fe FdIII (thick line), 25 μM. All samples are in 0.1 M potassium phosphate buffer, pH 7.4. FdIII is much smaller than FdI and therefore has a quite different ratio of A_{280} to A_{400}.

Spectroscopic Evidence for the Formation of a New [4Fe-4S]$^{2+/+}$ Cluster. Although native FdI is an air-stable protein, many [Fe-S] proteins, including some altered forms of FdI, are oxygen-sensitive. For that reason, as a precautionary measure, ΔT14/ΔD15 FdI was initially purified anaerobically. Figure 3 compares the UV−Vis absorption spectra of anaerobically oxidized ΔT14/ΔD15 FdI to that of native FdI, and to *A. vinelandii* FdIII which is known to contain two $[4Fe\text{-}4S]^{2+/+}$ clusters (*27*). The shape of the ΔT14/ΔD15 spectrum is very characteristic of 8Fe ferredoxins (*26*−*28*) and quite different from the spectrum exhibited by native FdI. The magnitude of the absorbance, however, is very similar for both proteins, indicating that there has been no loss of Fe in the ΔT14/ΔD15 variant. The ratio of A_{280}/A_{400} for several ΔT14/ΔD15 FdI preparations ranged from 1.6 to 1.8, very close to values previously reported for the native protein (*16*), leading to the conclusion that two [Fe-S] clusters must be present in ΔT14/ΔD15 FdI.

The CD spectra of native FdI, ΔT14/ΔD15 FdI, and FdIII from *A. vinelandii* are compared in Figure 4. Again the wavelength dependence and form of the mutant spectrum are very characteristic of spectra obtained for 8Fe ferredoxins (*26*−*28*) and quite different from native FdI. It is interesting to note, however, that the major feature in the A_{500} to A_{600} region appears to be very similar in magnitude and shape when comparing native and ΔT14/ΔD15 FdI or the 8Fe ferredoxin, suggesting that this feature arises primarily from the $[4Fe\text{-}4S]^{2+}$ cluster that is present in native FdI.

In general, the presence of an $S = 1/2$ $[4Fe\text{-}4S]^{+}$ cluster in a protein can be confirmed by the appearance of a characteristic anisotropic EPR signal with $g_{av} \sim 1.94$ (*29*). For native FdI, however, because of the very low reduction potential of its $[4Fe\text{-}4S]^{2+/+}$ cluster (*30*), the addition of excess dithionite at neutral pH reduces only the $[3Fe\text{-}4S]^{+}$ cluster (to the zero oxidation level) without reducing the $[4Fe\text{-}4S]^{2+}$ cluster. Thus, as shown in Figure 5a, the reduced spectrum for native FdI is EPR-silent (*16*). In contrast to this result for native FdI, the spectrum of dithionite-reduced ΔT14/ΔD15 (Figure 5b) exhibits an EPR signal, $g_{av} \sim 1.94$,

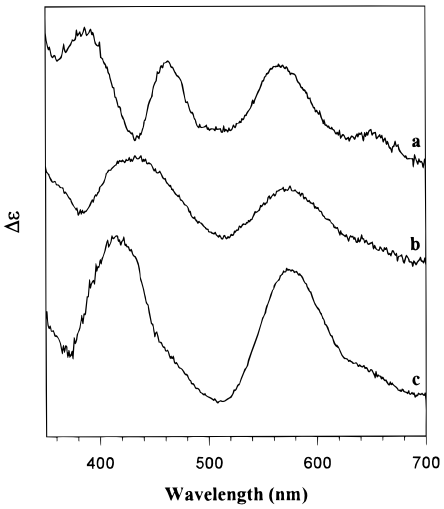

FIGURE 4: Visible region CD spectra of (a) native oxidized *Av*FdI (40 μM), (b) ΔT14/ΔD15 FdI (40 μM), and (c) the 8Fe FdIII (50 μM).

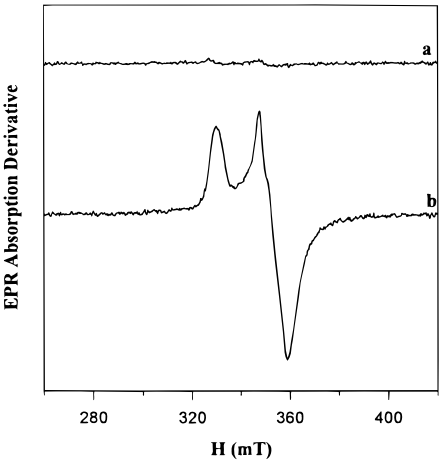

FIGURE 5: EPR spectra of (a) dithionite-reduced native *Av*FdI (11 K) and (b) dithionite-reduced ΔT14/ΔD15 FdI (13 K). The samples were 100 μM in 0.025 M Tris-HCl, pH 7.4, 2 mM sodium dithionite. The microwave power was 0.05 mW, the modulation amplitude was 5.1 G, and the microwave frequency was 9.43 GHz.

that arises from an $S = 1/2$ $[4Fe\text{-}4S]^{+}$ cluster and which integrates to >0.9 spin per molecule. The simplest explanation for this result is that this signal arises from the reduction of a new $[4Fe\text{-}4S]^{2+/+}$ cluster which now occupies the [3Fe-4S] position of native FdI. That only one of the two [4Fe-4S] clusters in the protein is being reduced by dithionite in these experiments is also illustrated in Figure 6 which shows that the extent of reduction of the native and ΔT14/ΔD15 FdI samples is the same. These data also lead to the conclusion that because it can be easily reduced by dithionite at neutral pH the new $[4Fe\text{-}4S]^{2+/+}$ cluster must have a reduction potential more positive than −480 mV versus the standard hydrogen electrode. Thus, even though the $[3Fe\text{-}4S]^{+/0}$ cluster of native FdI has a very negative potential for a cluster of that type, the new $[4Fe\text{-}4S]^{2+/+}$ cluster in the same position has a potential similar to the clusters found in the 8Fe clostridial-type ferredoxins (*31*).

Iron Content Analysis. Direct iron content analysis gives 7.64 ± 0.15 iron atoms per molecule, and in the same assay, the native 7Fe FdI and 8Fe FdIII give 7.00 ± 0.08 and 7.65 ± 0.62 Fe atoms per molecule, respectively.

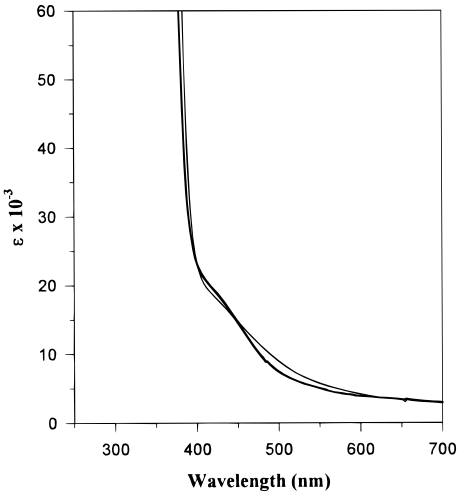

FIGURE 6: UV−visible absorption spectra of dithionite-reduced native *Av*FdI (thin line) and ΔT14/ΔD15 FdI (thick line) in 0.1 M potassium phosphate, pH 7.4, 2 mM dithionite. Both protein samples were 30 μM. The oxidized spectra are shown in Figure 3.

Electrochemistry. To confirm that ΔT14/ΔD15 FdI is an 8Fe protein and to investigate further the potentials of its two [4Fe-4S] clusters, direct electrochemical methods were employed. Figure 7A shows a voltammogram obtained at pH 7.0, 0 °C, for a solution of anaerobically isolated ΔT14/ΔD15 FdI (the principal and leading fractions observed by FPLC). Two redox couples, A and B, are observed, each conforming to expectations for a diffusion-controlled quasi-reversible electrode reaction (*21*); i.e., oxidation and reduction waves are of approximately equal size, and peak currents are dependent on the square root of the scan rate up to 20 mV s^{-1}. Reduction potentials determined from the average of oxidation and reduction peak potentials are −466 and −612 mV for A and B, respectively. Film voltammetry was performed to check for the presence of a [3Fe-4S] cluster, which normally yields a relatively narrow two-electron signal due to the complex proton-coupled 0/2− reaction at potentials in the region of −700 mV at pH 7 (*20*). Figure 7B shows a film voltammogram obtained for a sample of anaerobically isolated ΔT14/ΔD15 FdI. Two signals are observed, which are denoted A′ and B′ (the prime signifying film measurements). They show the typical properties of immobilized redox couples, with peak currents proportional to scan rate and peak separations close to 0 mV under slow conditions (*32*). The signals have approximately equal areas (after base line subtraction), with signal B′ being somewhat broader. Importantly, the characteristic feature (sharp peak or peaks at low potential) that would signify a $[3Fe\text{-}4S]^{0/2-}$ couple is absent. Reduction potentials for signals A′ and B′ are −478 and −642 mV. Use of different buffers, i.e., 20 mM HEPES instead of 60 mM mixed buffer, gave identical results. The pH dependencies of reduction potentials were also determined using film voltammetry. For this 8Fe form, voltammograms measured at pH 5.5 revealed little difference in potentials as compared to pH 7.0, and values of −470 and −640 mV were recorded for the A and B couples, respectively.

From the spectroscopic evidence described above, signals A (A′) and B (B′) in the voltammograms of the anaerobically prepared ΔT14/ΔD15 FdI are assigned to the two $[4Fe\text{-}4S]^{2+/+}$ clusters. The signal with $E^{0'} = -466$ mV corre-

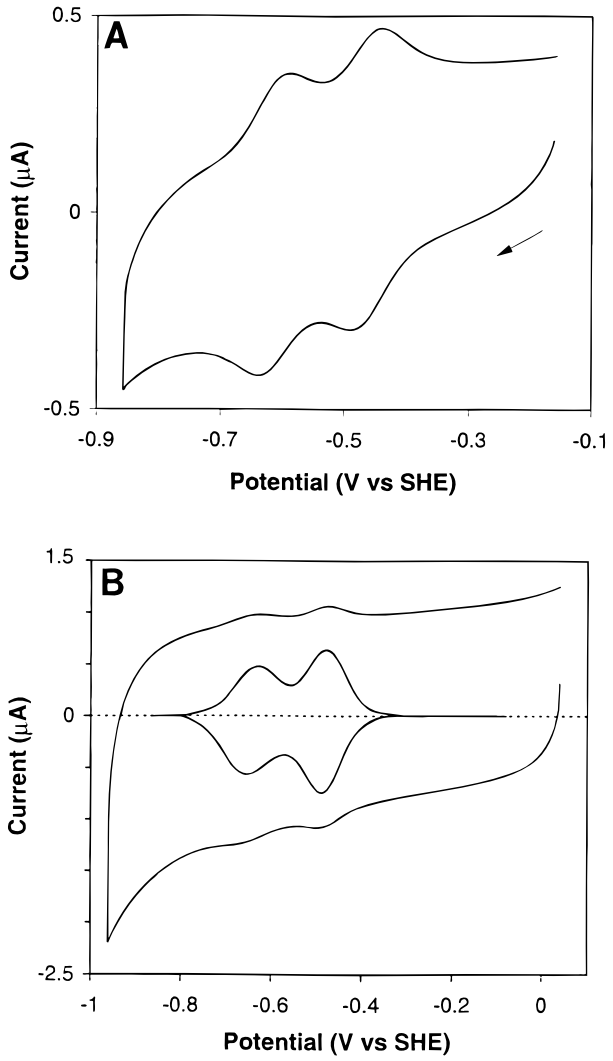

FIGURE 7: Voltammetry of ΔT14/ΔD15 FdI. (A) Voltammogram of a solution of ΔT14/ΔD15 FdI, 100 μM, in 20 mM HEPES, 0.1 M NaCl, pH 7.0, containing 3 mM neomycin, scan rate 5 mV s^{-1}, at 0 °C. (B) Film voltammogram of anaerobically purified ΔT14/ΔD15 FdI, scanned in 20 mM HEPES, 0.1 M NaCl, 0.1 mM EGTA, 200 μg/mL polymyxin B sulfate at pH 7.0, at 0 °C and scan rate 20 mV s^{-1}.

sponds to the new and dithionite-reducible cluster while the −642 mV signal arises from the unaltered [4Fe-4S]$^{2+/+}$ cluster present originally in native FdI. It is important to note that this new [4Fe-4S]$^{2+/+}$ cluster has an $E^{0'}$ very similar to that of the [3Fe-4S]$^{+/0}$ cluster in the native protein.

Summary of Results for the 8Fe Protein. Taken together, the spectroscopic and electrochemical data presented here establish that in ΔT14/ΔD15 FdI a new [4Fe-4S]$^{2+/+}$ cluster is created to replace the [3Fe-4S]$^{+/0}$ cluster present at the same position in the native FdI. These data show that it is sequence motif alone that is critical and sufficient for assembly of a 4Fe cluster in that region of the protein. That it is the motif, rather than the exact sequence, involving the presence of Gly and/or Ala residues between Cys residues that is important is shown by the sequence comparisons in Figures 1 and 2. These data also demonstrate that the C-terminal extension which makes *Av*FdI twice as long as the clostridial ferredoxins and wraps around the 3Fe portion of the protein does not prevent formation of a [4Fe-4S] cluster in the [3Fe-4S] region of the protein.

4Fe to 3Fe Cluster Conversion. Proteins that contain [3Fe-4Fe]$^{+/0}$ clusters can be divided into two general categories depending upon whether the 3Fe cluster can be converted to a 4Fe cluster easily simply by adding Fe^{2+} under reducing conditions. Proteins in the easy to convert category include *Desulfovibrio gigas* FdII (*33*), *D. africanus* FdIII (*34*), *Pyrococcus furiosis* Fd (*35*), and aconitase (*36*). In the case of *D. gigas* FdII, an X-ray structure of the [3Fe-4S]$^{+}$ form of the protein revealed that the cluster is ligated by cysteine residues 8, 14, and 50, while a free cysteine is present at position 11 to give the CysXXCysXXCys motif typical of [4Fe-4S] clusters. However, the second cysteine at position 11 is rotated away from the cluster and appears to be covalently modified by a methanethiol group, preventing it from serving as a ligand (*37*). In the cases of *D. africanus* FdIII (*34*, *38*) and *P. furiosis* Fd (*35*), the [4Fe-4S] CysXXCysXXCys motif has been changed to a CysXX-AspXXCys motif. Upon reduction and the addition of Fe^{2+}, a [4Fe-4S]$^{2+/+}$ cluster is formed, and it appears that the new ligand is supplied by aspartate (*39*−*41*). For aconitase, the fourth ligand is also known to be OH^- (or H_2O) (*42*, *43*).

Mutagenesis experiments involving other proteins have also been successful in converting a 4Fe cluster to a 3Fe cluster by mutating the second cysteine of a CysXXCysXX-Cys sequence to a nonligating residue (*44*, *45*) and in converting a 3Fe cluster to a 4Fe cluster by mutating a non-cysteine residue in the central position into a cysteine (*46*−*48*). Unlike the proteins just discussed, native *Av*FdI does not have a CysXXCys(or other residue)XXCys sequence. Also, unlike those proteins, the 3Fe cluster of native *Av*FdI does not easily convert to a 4Fe cluster. An 8Fe form of *Av*FdI has been reported, but its creation requires either complete denaturation to form apoprotein, followed by refolding in the presence of iron and sulfide (*49*), or the addition of the denaturing agent guanidine hydrochloride to the 7Fe protein (*50*). The structure of that 8Fe variant of FdI is not yet available, and, therefore, the nature of the fourth ligand has not been established, although it is likely to be Cys 11 (*50*).

For 8Fe or 4Fe ferredoxins that normally contain only [4Fe-4S]$^{2+/+}$ clusters (*26*, *27*, *51*), for the 8Fe variant of *Av*FdI created by chemical modification (*49*, *50*), and for new [4Fe-4S]$^{2+/+}$ clusters created by replacing an Asp and introducing a new Cys ligand into the central position of a CysXXAspXXCys motif (*46*, *47*), conversion of the new 4Fe cluster back to a 3Fe cluster is not facile. Addition of oxygen or ferricyanide to these proteins gives either no 3Fe or poor yields of 3Fe cluster followed by denaturation and loss of the cluster. This result is also obtained for the 8Fe ΔT14/ΔD15 FdI. Figure 8 shows that air oxidation of ΔT14/ΔD15 FdI does lead to formation of a $g = 2.01$ signal arising from a [3Fe-4S]$^{+}$ cluster that is very similar in g value and shape to that of the oxidized native FdI, and the power and temperature dependencies are also indistinguishable. However, a direct comparison of the magnitude of the two signals shown in Figure 8 indicates that the yield is only about 20%. Longer term exposure leads to protein denaturation and complete destruction of both clusters.

To obtain additional information about this 7Fe form of ΔT14/ΔD15 FdI, we took a sample of the 8Fe protein, exposed it to air, and then subjected it to anaerobic FPLC immediately prior to carrying out direct electrochemical

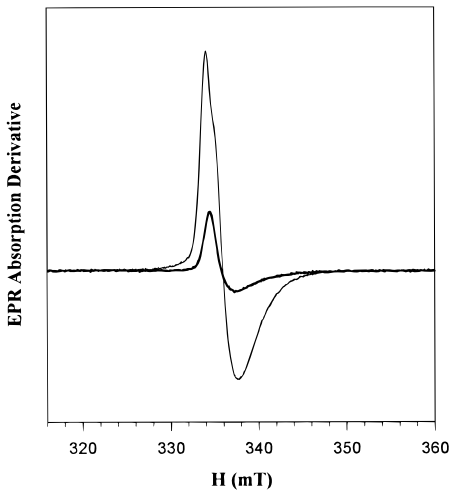

FIGURE 8: EPR spectra of native FdI (thin line) and ΔT14/ΔD15 FdI (thick line) at 11 K following 20 min of air oxidation in 0.025 M Tris-HCl, pH 7.4. Both samples were 100 μM, and gains were identical. The ΔT14/ΔD15 FdI signal integrates to 20% of the native FdI signal. The microwave power was 0.05 mW, the modulation amplitude was 5.1G, and the microwave frequency was 9.43 GHz.

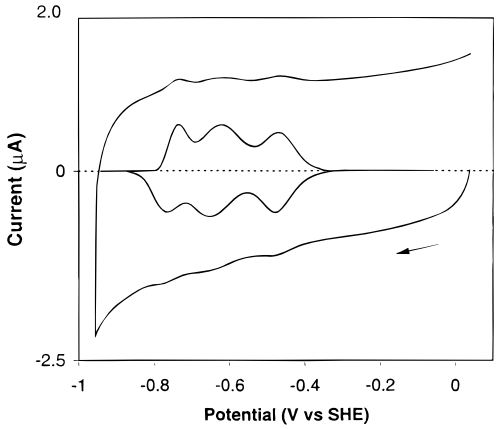

FIGURE 9: Film voltammogram of aerobically treated ΔT14/ΔD15 FdI, scanned in 60 mM mixed buffer, 0.1 M NaCl, 0.1 mM EGTA, 200 μg/mL polymyxin B sulfate at pH 7.0, at 0 °C and scan rate 20 mV s^{-1}. The relative attenuation of signal C′ compared to A′ and B′ (these integrate to approximately equal areas) is due to the presence in the aerobic sample of some 8Fe Fd which we could not completely separate. For a pure sample of 7Fe ferredoxin, signals A′, B′, and C′ should integrate in the ratio 1:1:2 (*20*).

experiments. Figure 9 shows a film voltammogram obtained at pH 7.0 for such a sample of ΔT14/ΔD15 FdI. In this case, three signals are observed, A′, B′, and C′, which have reduction potentials of −478, −636, and −748 mV, respectively. The aerobically prepared sample displays the characteristic sharp signal of a [3Fe-4S]$^{0/2-}$ cluster (C′). As now established for several proteins, the [3Fe-4S] cluster exhibits proton-coupled redox equilibria (*20*, *30*, *52*). As expected, there was a marked pH dependence of the reduction potential of this signal C′, with a decrease from −748 mV at pH 7.0 to −634 mV at pH 5.0 being clearly observable (*20*).

Taken together, the electrochemical results shown in Figure 9 confirm the presence of the [3Fe-4S] cluster in the aerobically treated and FPLC-purified sample. From their similarity between the different samples, and based upon results obtained for other mutant forms of *Av*FdI (*15*, *17*, *30*), signals B (B′) in both aerobic (Figure 9) and anaerobic (Figure 7A,B) samples are assigned to the unmutated [4Fe-4S] cluster. Signals A and A′ are coincidental in both aerobic and anaerobic samples, the [3Fe-4S]$^{+/0}$ and [4Fe-4S]$^{2+/+}$ clusters formed in either case having reduction potentials sufficiently close that they cannot be resolved by voltammetry. A major conclusion from this study is therefore that the [3Fe-4S]$^{+/0}$ cluster of 7Fe ΔT14/ΔD15 FdI has a reduction potential extremely similar to that of the new [4Fe-4S]$^{2+/+}$ cluster in the same position of 8Fe ΔT14/ΔD15 FdI. This is in contrast to the expectations that the two different types of clusters at the same position should have very different reduction potentials (*31*, *41*, *47*, *53*−*55*). Indeed, in those ferredoxins that contain reversibly interconvertible [4Fe-4S]$^{2+/+}$ and [3Fe-4S]$^{+/0}$ clusters, the two clusters always have widely differing reduction potentials, with the potential of the [3Fe-4S]$^{+/0}$ cluster being more positive than that of the [4Fe-4S]$^{2+/+}$ cluster by 180−260 mV (*33*, *41*, *47*, *53*−*55*). The facility and reversibility of the cluster conversions in these proteins may suggest that there are no major structural rearrangements around the clusters during the cluster converison and the two clusters formed in the same position share a similar environment. In contrast, the extensive rearrangement in ΔT14/ΔD15 FdI as suggested by the structural analysis would lead to an environment around the newly formed [4Fe-4S] cluster which is very different from that around the [3Fe-4S] cluster in the native protein. In this sense, the similarity in the reduction potentials between the two clusters may be coincidental. Future structural characterization of ΔT14/ΔD15 FdI should shed light on our understanding of the factors that affect and determine the reduction potentials of these [Fe-S] clusters.

Physiological Considerations. *A. vinelandii* FdI has an electron-transfer function in a metabolic process that is unrelated to N_2 fixation but which is important for cell growth (*56*). In previous studies, we have shown that the 7Fe form of FdI is not an artifact of aerobic isolation of the protein, and that when expressed in *A. vinelandii*, even subtle mutations near the 3Fe cluster have a serious negative effect on the growth rate of the cell (*17*). Figure 10 shows for the first time that the oxidized 3Fe cluster EPR signal can be easily observed in whole cells. This result again emphasizes the physiological relevance of the 3Fe center. The observation that the 3Fe center is important, however, does not preclude the possibility that an 8Fe version of the protein may be physiologically relevant. Indeed, reconstitution of apo FdI does lead to an 8Fe form in vitro (*49*), and as discussed above, a method has been developed for conversion of 7Fe FdI to 8Fe FdI in vitro (*50*). Here we have constructed an 8Fe variant of FdI by site-directed mutagenesis and have expressed the protein in its native background in *A. vinelandii*. The whole-cell EPR data shown in Figure 10 confirm that the 7Fe protein is not present in cells expressing ΔT14/ΔD15 FdI. The strain expressing the ΔT14/ΔD15 FdI has a much longer lag phase and a much slower growth rate during the log phase than the strain expressing native FdI. These data suggest that the 8Fe variant is defective in the in vivo electron-transfer function, again emphasizing the importance of the 3Fe cluster for this function.

In addition to its electron-transfer function, FdI has a regulatory function in controlling the expression of the *fpr* gene product, NADPH:ferredoxin reductase (*56*−*59*). Like native FdI (*56*−*59*), ΔT14/ΔD15 FdI is still capable of

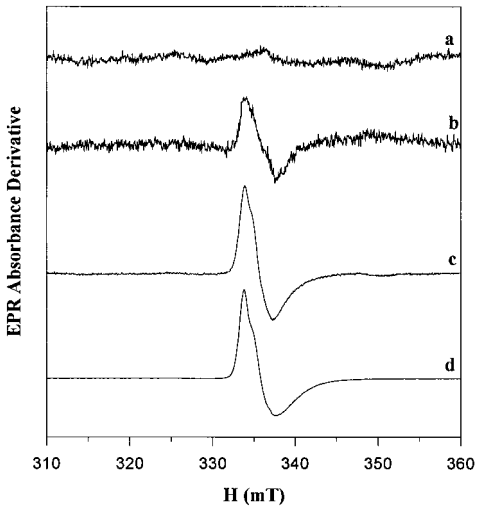

FIGURE 10: EPR spectra of concentrated *A. vinelandii* cultures at 10 K. (a) The ΔT14/ΔD15 FdI mutant variant; (b) *Av*OP, the wild-type strain expressing native FdI; (c) pDB214, the wild-type FdI overexpression strain (*69*); and (d) purified native *Av*FdI in 0.025 M Tris-HCl, pH 7.4, at 100 μM. The microwave power was 0.5 mW, the modulation amplitude was 5.1 G, and the microwave frequency was 9.43 GHz. The levels of FdI in (a) and (b) are equivalent as determined both by Western analysis of cell-free extracts and by protein purification yields.

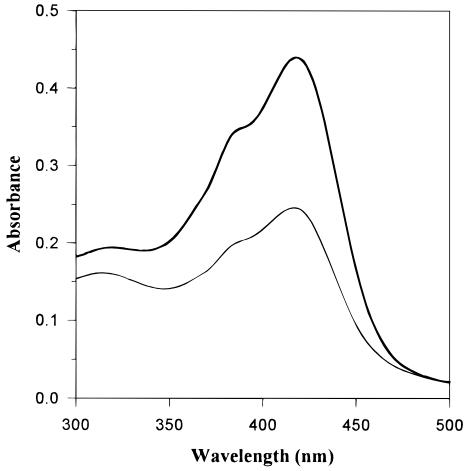

FIGURE 11: Comparison of Azotobactin D levels produced by strains overproducing native *Av*FdI (thin line) and ΔT14/ΔD15 FdI (thick line). Cells were grown under identical N_2-fixing conditions in the presence of limited iron (0.1 μM Fe^{3+}). The absorbance maximum at 380 μM is due to Azotobactin D without iron, and the absorbance maximum at 418 μM is due to Azotobactin D with Fe(III) bound (*70*, *71*).

carrying out that regulatory function such that FPR levels in the strains overproducing those two proteins are equivalent. We did, however, consistently notice a difference in the growth of the ΔT14/ΔD15 strain that may be related to the regulatory function of FdI. As shown in Figure 11, the ΔT14/ΔD15 FdI strain appears to overproduce the siderophore Azotobactin D such that the levels of Azotobactin D are the same in the ΔT14/ΔD15 FdI and the native FdI producing strains when the mutant strain has an order of magnitude more iron present. In other words, the cells appear to respond as if they have less iron than is really available. This new manifestation of the regulatory function of FdI is under further investigation, but it is interesting to note that this is the only mutant we have produced to date that appears to be present in an 8Fe form in vivo, and it is also the only one that appears to overproduce Azotobactin D.

CONCLUSION

We have demonstrated the generation of the first example of a stable 8Fe *Av*FdI. The creation of a $[4Fe\text{-}4S]^{2+/+}$ cluster at the position of the $[3Fe\text{-}4S]^{+/0}$ cluster in the native protein is accomplished by introducing a highly conserved $[4Fe\text{-}4S]^{2+/+}$ cluster-binding Cys motif, CysXXCysXXCysXXX-CysPro, without modifying residues between the cysteines to include the Gly and/or Ala residue(s) normally present and without removing the C-terminal extension that wraps around that portion of the protein. The newly formed [4Fe-4S] cluster converts to a [3Fe-4S] cluster in very low yield. Unlike all previous examples of 3Fe to 4Fe cluster conversions, the native $[3Fe\text{-}4S]^{+/0}$ cluster, the new $[4Fe\text{-}4S]^{2+/+}$ cluster, and the $[3Fe\text{-}4S]^{+/0}$ cluster, resulted from oxidation of the ΔT14/ΔD15 FdI, all have extremely similar reduction potentials. Data and structural models suggest major structural rearrangements around this [4Fe-4S] cluster in the ΔT14/ΔD15 FdI compared to the native protein. The formation of the new [4Fe-4S] cluster may have altered the physiological activity of FdI and may be the basis of the significantly altered siderophore production in this mutant.

ACKNOWLEDGMENT

We thank Dr. Dave Stout, Scripps Research Institute, for his helpful discussion concerning the structural analysis.

REFERENCES

1. Bruschi, M., and Guerlesquin, F. (1988) *FEMS Microbiol. Rev. 54*, 155−175.
2. Johnson, M. K. (1994) in *Encyclopedia of Inorganic Chemistry* (King, R. B., Ed.) Vol. 4, pp 1896−1915, Wiley, Chichester, England.
3. Howard, J., and Rees, D. C. (1991) *Adv. Protein Chem. 42*, 199−280.
4. Beinert, H. (1990) *FASEB J. 4*, 2483−2491.
5. Lindahl, P. A., and Kovacs, J. A. (1990) *J. Cluster Sci. 1*, 29−73.
6. Holm, R. H., Kennepohl, P., and Solomon, E. I. (1996) *Chem. Rev. 96*, 2239−2314.
7. Beinert, H., Holm, R. H., and Münck, E. (1997) *Science 277*, 653−659.
8. Stout, G. H., Turley, S., Sieker, L. C., and Jensen, L. H. (1988) *Proc. Natl. Acad. Sci. U.S.A. 85*, 1020−1022.
9. Stout, C. D. (1988) *J. Biol. Chem. 263*, 9256−9260.
10. Stout, C. D. (1989) *J. Mol. Biol. 205*, 545−555.
11. Merritt, E. A., Stout, G. H., Turley, S., Sieker, L. C., Jensen, L. H., and Orme-Johnson, W. H. (1993) *Acta Crystallogr. D49*, 272−281.
12. Adman, E. T., Sieker, L. C., and Jensen, L. H. (1973) *J. Biol. Chem. 248*, 3987−3996.
13. Adman, E. T., Sieker, L. C., and Jensen, L. H. (1976) *J. Biol. Chem. 251*, 3801−3806.
14. Backes, G., Mino, Y., Loehr, T. M., Meyer, T. E., Cusanovich, M. A., Sweeney, W. V., Admon, E. T., and Sanders-Loehr, J. (1991) *J. Am. Chem. Soc. 113*, 2055−2064.
15. Kemper, M. A., Stout, C. D., Lloyd, S. J., Prasad, G. S., Fawcett, S. E. J., Armstrong, F. A., Shen, B., and Burgess, B. K. (1997) *J. Biol. Chem. 272*, 15620−15627.
16. Stephens, P. J., Jensen, G. M., Devlin, F. J., Morgan, T. V., Stout, C. D., Martin, A. E., and Burgess, B. K. (1991) *Biochemistry 30*, 3200−3209.

17. Shen, B., Martin, L. L., Butt, J. N., Armstrong, F. A., Stout, C. D., Jensen, G. M., Stephens, P. J., La Mar, G. N., Gorst, C. M., and Burgess, B. K. (1993) *J. Biol. Chem. 268*, 25928−25939.
18. Morgan, T. V., Lundell, D. J., and Burgess, B. K. (1988) *J. Biol. Chem. 263*, 1370−1375.
19. Burgess, B. K., Jacobs, D. B., and Stiefel, E. I. (1980) *Biochim. Biophys. Acta 614*, 196−209.
20. Duff, J. L. C., Breton, J. L. J., Butt, J. N., Armstrong, F. A., and Thomson, A. J. (1996) *J. Am. Chem. Soc. 118*, 8593−8603.
21. Bard, A. J., and Faulkner, L. R. (1980) in *Electrochemical Methods: Fundamentals and Applications*, Wiley, New York.
22. Armstrong, F. A. (1997) in *Bioelectrochemistry of Biomacromolecules: Bioelectrochemistry: Principles and Practice* (Lenaz, G., and Milazzo, G., Eds.) pp 205−255, Birkhauser Verlag, Basel.
23. Shen, B., Jollie, D. R., Stout, C. D., Diller, T. C., Armstrong, F. A., Gorst, C. M., La Mar, G. N., Stephens, P. J., and Burgess, B. K. (1994) *J. Biol. Chem. 269*, 8564−8575.
24. Martín, A. E., Burgess, B. K., Stout, C. D., Cash, V. L., Dean, D. R., Jensen, G. M., and Stephens, P. J. (1990) *Proc. Natl. Acad. Sci. U.S.A. 87*, 598−602.
25. Shen, B., Jollie, D. R., Diller, T. C., Stout, C. D., Stephens, P. J., and Burgess, B. K. (1995) *Proc. Natl. Acad. Sci. U.S.A. 92*, 10064−10068.
26. Reyntjens, B., Jollie, D. R., Stephens, P. J., Gao-Sheridan, H. S., and Burgess, B. K. (1997) *J. Biol. Inorg. Chem. 2*, 595−602.
27. Gao-Sheridan, H. S., Pershad, H. R., Armstrong, F. A., and Burgess, B. K. (1998) *J. Biol. Chem. 273*, 5514−5519.
28. Stephens, P. J., Thomson, A. J., Dunn, J. B., Keiderling, T. A., Rawlings, J., Rao, K. K., and Hall, D. O. (1978) *Biochemistry 17*, 4770−4778.
29. Orme-Johnson, W. H., and Sands, R. H. (1973) in *Iron−sulfur proteins II* (Lovenberg, W., Ed.) pp 195−238, Academic Press, New York.
30. Iismaa, S. E., Vázquez, A. E., Jensen, G. M., Stephens, P. J., Butt, J. N., Armstrong, F. A., and Burgess, B. K. (1991) *J. Biol. Chem. 266*, 21563−21571.
31. Stephens, P. J., Jollie, D. R., and Warshel, A. (1996) *Chem. Rev. 96*, 2491−2513.
32. Laviron, E. (1982) in *Electroanalytical Chemistry* (Bard, A. J., Ed.) Vol. 12, pp 53−157, Marcel Dekker, New York.
33. Moura, J. J. G., Moura, I., Kent, T. A., Lipscomb, J. D., Huynh, B. H., LeGall, J., Xavier, A. V., and Münck, E. (1982) *J. Biol. Chem. 257*, 6259−6267.
34. George, S. J., Armstrong, F. A., Hatchikian, E. C., and Thomson, A. J. (1989) *Biochem. J. 264*, 275−284.
35. Conover, R. C., Kowal, A. T., Fu, W., Park, J. B., Aono, S., Adams, M. W., and Johnson, M. K. (1990) *J. Biol. Chem. 265*, 8533−8541.
36. Beinert, H., and Kennedy, M. C. (1989) *Eur. J. Biochem. 186*, 5−15.
37. Kissinger, C. R., Sieker, L. C., Adman, E. T., and Jensen, L. H. (1991) *J. Mol. Biol. 219*, 693−715.
38. Thomson, A. J., Breton, J., Butt, J. N., Hatchikian, E. C., and Armstrong, F. A. (1992) *J. Inorg. Biochem. 47*, 197−207.
39. Gorst, C. M., Yeh, Y. H., Teng, Q., Calzolai, L., Zhou, Z. H., Adams, M. W., and La Mar, G. N. (1995) *Biochemistry 34*, 600−610.
40. Calzolai, L., Gorst, C. M., Zhao, Z., Teng, Q., Adams, M. W., and La Mar, G. N. (1995) *Biochemistry 34*, 11373−11384.
41. Calzolai, L., Zhou, Z. H., Adams, M. W., and La Mar, G. N. (1996) *J. Am. Chem. Soc. 118*, 2513−2514.
42. Robbins, A. H., and Stout, C. D. (1989a) *Proc. Natl. Acad. Sci. U.S.A. 86*, 3639−3643.
43. Robbins, A. H., and Stout, C. D. (1989b) *Proteins: Struct., Funct., Genet. 5*, 289−312.
44. Rothery, R. A., and Weiner, J. H. (1991) *Biochemistry 30*, 8296−8305.
45. Zhao, J., Li, N., Warren, P. V., Golbeck, J. H., and Bryant, D. A. (1992) *Biochemistry 31*, 5093−5099.
46. Manodori, A., Cecchini, G., Schroder, I., Gunsalus, R. P., Werth, M. T., and Johnson, M. K. (1992) *Biochemistry 31*, 2703−2712.
47. Busch, J. L. H., Breton, J. L., Bartlett, B. M., Armstrong, F. A., James, R., and Thomson, A. J. (1997) *Biochem. J. 323*, 95−102.
48. Aono, S., Bentrop, D., Bertini, I., Luchinat, C., and Macinai, R. (1997) *FEBS Lett. 412*, 501−505.
49. Morgan, T. V., Stephens, P. J., Burgess, B. K., and Stout, C. D. (1984) *FEBS Lett. 167*, 137−141.
50. Jensen, G. M. (1994) Ph.D. Dissertation, University of Southern California, pp 106−156.
51. Thomson, A. J., Robinson, A. E., Johnson, M. K., Cammack, R., Rao, K. K., and Hall, D. O. (1981) *Biochim. Biophys. Acta 637*, 423−432.
52. Breton, J. L., Duff, J. L. C., Butt, J. N., Armstrong, F. A., George, S. J., Pétillot, Y., Forest, E., Schäfer, G., and Thomson, A. J. (1995) *Eur. J. Biochem. 233*, 937−946.
53. Asso, M., Mbarki, O., Guigliarelli, B., Yagi, T., and Bertrand, P. (1995) *Biochem. Biophys. Res. Commun. 211*, 198−204.
54. Zhou, Z. H., and Adams, M. W. (1997) *Biochemistry 36*, 10892−10900.
55. Tong, J., and Feinberg, B. A. (1994) *J. Biol. Chem. 269*, 24920−24927.
56. Martín, A. E., Burgess, B. K., Iismaa, S. E., Smartt, C. T., Jacobson, M. R., and Dean, D. R. (1989) *J. Bacteriol. 171*, 3162−3167.
57. Isas, J. M., and Burgess, B. K. (1994) *J. Biol. Chem. 269*, 19404−19409.
58. Isas, J. M., Yannone, S. M., and Burgess, B. K. (1994) *J. Biol. Chem. 270*, 21258−21263.
59. Yannone, S. M., and Burgess, B. K. (1997) *J. Biol. Chem. 272*, 14454−14458.
60. Quinkal, I., Davasse, V., Gaillard, J., and Moulis, J. M. (1994) *Protein Eng. 7*, 681−687.
61. Graves, M. C., Mullenbach, G. T., and Rabinowitz, J. C. (1985) *Proc. Natl. Acad. Sci. U.S.A. 82*, 1653−1657.
62. Hase, T., Wakabayashi, S., and Matsubara H. (1978) *FEBS Lett. 91*, 315−319.
63. Saeki, K., Wakabayashi, S., Zumft, W. G., and Matusbara, H. (1988) *J. Biochem. 104*, 242−246.
64. Saeki, K., Suetsugu, Y., Yao, Y., Horio, T., Marrs, B. L., and Matusbara, H. (1990) *J. Biochem. 108*, 475−482.
65. Wang, S. P., Kang, P. J., Chen, Y. P., and Ely, B. (1995) *J. Bacteriol. 177*, 2901−2907.
66. Aono, S., Nakamura, S., Aono, R., and Okura, I. (1994) *Biochem. Biophys. Res. Commun. 201*, 938−942.
67. Trower, M. K., Marshall, J. E., Doleman, M. S., Emptage, M. H., and Sariaslani, F. S. (1990) *Biochim. Biophys. Acta 1037*, 290−296.
68. Sato, S., Nakazawa, K., Hon-Nami, K., and Oshima, T. (1981) *Biochim. Biophys. Acta 668*, 277−281.
69. Vásquez, A., Shen, B., Negaard, K., Iismaa, S., and Burgess B. K. (1994) *Protein Overexpression Purif. 5*, 96−102.
70. Demange, P., Wendenbaum, S., Bateman, A., Dell, A., and Abdallah, M. A. (1987) in *Iron Transport in Microbes, Plants and Animals* (Winkelman, G., van der Helm, D., and Neilands, J. B., Eds.) pp 167−188, VCH, Federal Republic of Germany.
71. Demange, P., Wendenbaum, S., Bateman, A., Dell, A., Meyer, J. M., and Abdallah, M. A. (1985) in *Iron, Siderophores, and Plant Diseases* (Swinburne, T. R., Ed.) pp 131−154, Plenum Press, New York.

BI9810499